environmental microbiology

Environmental Microbiology (2021) **00**(00), 00–00 doi:10.1111/1462-2920.15816

Escherichia coli cryptic prophages sense nutrients to influence persister cell resuscitation

Sooyeon Song,[1,2,3] Jun-Seob Kim,[4] Ryota Yamasaki,[5] Sejong Oh,[6] Michael J. Benedik[7] and Thomas K. Wood[1*]

[1]*Department of Chemical Engineering, Pennsylvania State University, University Park, Pennsylvania, 16802-4400.*

[2]*Department of Animal Science, Jeonbuk National University, 587 Baekje-Daero, Deokjin-Gu, Jeonju-Si, Jeollabuk-Do, 54896, South Korea.*

[3]*Department of Agricultural Convergence Technology, Jeonbuk National University, 587 Baekje-Daero, Deokjin-Gu, Jeonju-Si, Jeollabuk-Do, 54896, South Korea.*

[4]*Department of Nano-Bioengineering, Incheon National University, 119 Academy-ro, Incheon, 22012, South Korea.*

[5]*Department of Health Promotion, Kyushu Dental University, Kitakyushu, Fukuoka, 803-8580, Japan.*

[6]*Division of Animal Science, Chonnam National University, 77 Yongbong-Ro, Buk-Gu, Gwangju, 61186, South Korea.*

[7]*Department of Biology, Texas A&M University, College Station, TX, 77843.*

Summary

Cryptic prophages are not genomic junk but instead enable cells to combat myriad stresses as an active stress response. How these phage fossils affect persister cell resuscitation has, however, not been explored. Persister cells form as a result of stresses such as starvation, antibiotics and oxidative conditions, and resuscitation of these persister cells likely causes recurring infections such as those associated with tuberculosis, cystic fibrosis and Lyme disease. Deletion of each of the nine *Escherichia coli* cryptic prophages has no effect on persister cell formation. Strikingly, elimination of each cryptic prophage results in an increase in persister cell resuscitation with a dramatic increase in resuscitation upon deleting all nine prophages. This increased resuscitation includes eliminating the need for a carbon source and is due to activation of the phosphate import system resulting from inactivating the transcriptional regulator AlpA of the CP4-57 cryptic prophage. Deletion of *alpA* increases persister resuscitation, and AlpA represses phosphate regulator PhoR. Both phosphate regulators PhoP and PhoB stimulate resuscitation. This suggests a novel cellular stress mechanism controlled by cryptic prophages: regulation of phosphate uptake which controls the exit of the cell from dormancy and prevents premature resuscitation in the absence of nutrients.

Introduction

The role cryptic prophages, which are trapped lysogens that no longer form active phage particles, play in the physiology of the host remains uncertain. Rather than merely being extraneous but stable DNA, comprising up to 20% of the genome (Casjens, 2003), the nine cryptic prophages of *E. coli* K-12 increase resistance to sublethal concentrations of quinolone and β-lactam antibiotics as well as protect the cell from osmotic, oxidative and acid stresses (Wang *et al*., 2010). Hence, the genome of a parasite has become interwoven into the bacterial genome and serves beneficial roles related to stress resistance (Wang *et al*., 2010). Since the extreme stress response of the cell population is for a small percentage of cells to become dormant (i.e. persistent) (Yamasaki *et al*., 2020) and cryptic prophages are utilized for an active stress response (Wang *et al*., 2010), it seems reasonable to consider that cryptic prophages may play a role in persistence; i.e. cryptic prophages may be involved in the extreme stress response.

Persister cells are phenotypic variants that arise without genetic change as a result of myriad stresses such as nutrient, antibiotic and oxidative stress (Hong *et al*., 2012; Kim *et al*., 2018a). Most cells in the stressed population mount an active response but the small subpopulation of persisters survive stresses by sleeping through the insults (Lewis, 2008). Since nearly all cells starve, the persister state is probably a universal resting state (Song and Wood, 2018). Critically, persister cells are likely the cause of many recurring infections (Van

Received 7 June, 2021; accepted 7 October, 2021. *For correspondence. E-mail tuw14@psu.edu; Tel. (+)1 814-863-4811; Fax (1) 814-865-7846.

© 2021 Society for Applied Microbiology and John Wiley & Sons Ltd.

den Bergh *et al*., 2017); therefore, understanding how they resuscitate is vital.

Persister cells can form as a result of translation inhibition. Specifically, by inhibiting transcription via sub-lethal concentrations of rifampicin, by inhibiting translation via sub-lethal concentrations tetracycline, or by interrupting translation by ceasing ATP production via carbonyl cyanide *m*-chlorophenyl hydrazone, we converted nearly all of the exponentially growing *E. coli* cells into persister cells (Kwan *et al*., 2013). To reduce protein production during stress, there is consensus (Korch *et al*., 2003; Nguyen *et al*., 2011; Chowdhury *et al*., 2016) for a role of the alarmone guanosine pentaphosphate/tetraphosphate (henceforth ppGpp) for forming persisters (Svenningsen *et al*., 2019); for example, by reducing transcription of ribosomal operons (Shimada *et al*., 2013). The ppGpp ribosome dimerization persister model proposes that ppGpp generates persister cells directly by inactivating ribosomes through the conserved ribosome hibernation factors RMF, HpF and RaiA which convert active 70S ribosomes into inactive 70S and 100S ribosomes (Song and Wood, 2020a, 2020b; Wood and Song, 2020). Persister cells were found to contain a large fraction of 100S ribosomes; inactivation of RMF, HpF and RaiA reduces persistence and increases single-cell persister resuscitation; and single-cell persister resuscitation does not depend on ppGpp. This model does not rely on toxin/antitoxin systems for persister cell formation as their direct link to persistence is tenuous (Goormaghtigh *et al*., 2018).

Persister cells resuscitate in a heterogeneous manner as they recognize external nutrients; the rate of resuscitation depends on the number of active ribosomes, and the growth rate of the resuscitated cells is exponential like the wild-type (Kim *et al*., 2018b). Later studies have verified this heterogeneous nature of persister cell resuscitation (Goormaghtigh and Van Melderen, 2019; Pu *et al*., 2019) and subsequent exponential growth of resuscitating cells (Mohiuddin *et al*., 2020); together, these later studies corroborate our method of forming persister cells. By screening 10 000 compounds for persister cell resuscitation, ribosomes were shown to be activated during persister cell resuscitation by pseudouridine synthase RluD that modifies 23S subunits (Song and Wood, 2020b). Resuscitation is initiated by recognizing external nutrients through receptors for chemotaxis (for amino acids) and phosphotransferase membrane proteins (for glucose) (Yamasaki *et al*., 2020). The external nutrient signals are propagated to the cytosol by reducing concentrations of the secondary messenger cAMP which leads to the rescue of stalled ribosomes and to the dissociation of inactive dimerized 100S ribosomes (Yamasaki *et al*., 2020). The resuscitating cells also initiate chemotaxis toward fresh nutrients since nutrient depletion triggered persistence (Yamasaki *et al*., 2020).

Here we explore the role of cryptic prophages in persister cell formation and resuscitation. To link cryptic prophages to stress resistance, a Δ9 strain was used in which all nine cryptic prophage elements (166 kb) of *E. coli* were precisely deleted, along with the set of nine single strains with each having one cryptic prophage deleted (Wang *et al*., 2010). Cryptic prophages are shown to not play a role in persister cell *formation* but instead reduce persister cell *resuscitation* and prevent resuscitation until a carbon source is present. By employing a whole transcriptome study to explore the impact of cryptic prophages on resuscitating cells, the cryptic prophages are shown to reduce resuscitation by repressing phosphate transport. Moreover, this phosphate transport system is repressed in part via the CP4-57 cryptic prophage regulator AlpA; specifically, AlpA represses *phoR*, which leads to activation of *phoB* and *pstB*. Hence, we discovered a novel physiological role for cryptic prophages, regulation of persister cell resuscitation and determined that the mechanism is through their regulation of phosphate sensing.

Results

Cryptic prophages do not affect persister cell formation

To determine whether cryptic prophages affect persister cell formation, we converted the wild-type, the Δ9 strain with all nine cryptic prophages deleted (Wang *et al*., 2010), and each single cryptic prophage mutant (Wang *et al*., 2010) to persister cells using a rifampicin pretreatment (Kwan *et al*., 2013) and enumerated them. This method of generating persister cells has been validated eight ways (Kim *et al*., 2018b) and utilized by at least 15 independent labs to date (Johnson and Levin, 2013; Kwan *et al*., 2013; Grassi *et al*., 2017; Cui *et al*., 2018; Jin *et al*., 2018; Narayanaswamy *et al*., 2018; Sulaiman *et al*., 2018; Tkhilaishvili *et al*., 2018; Pu *et al*., 2019; Martins *et al*., 2020; Rowe *et al*., 2020; Sun *et al*., 2020; Yu *et al*., 2020; Zhao *et al*., 2020; Zheng *et al*., 2020); the approach has the benefit of increasing the number of persister cells by 10 000-fold (Kwan *et al*., 2013) which enables single-cell studies (Kim *et al*., 2018a; Kim *et al*., 2018b; Song and Wood, 2020a; Yamasaki *et al*., 2020).

Using this rifampicin-pretreatment method, the presence of the cryptic prophages was shown to have no significant impact on the number of persister cells formed with ampicillin since the differences between strains were less than twofold and important changes in persister levels usually result in at least changes of several magnitudes (Fig. 1). Corroborating this result, ATP levels for persister cells were similar for both the wild-type and the Δ9 strain (Table S1); previously, we demonstrated reducing ATP levels increases persistence by 10 000-fold with

© 2021 Society for Applied Microbiology and John Wiley & Sons Ltd., *Environmental Microbiology*

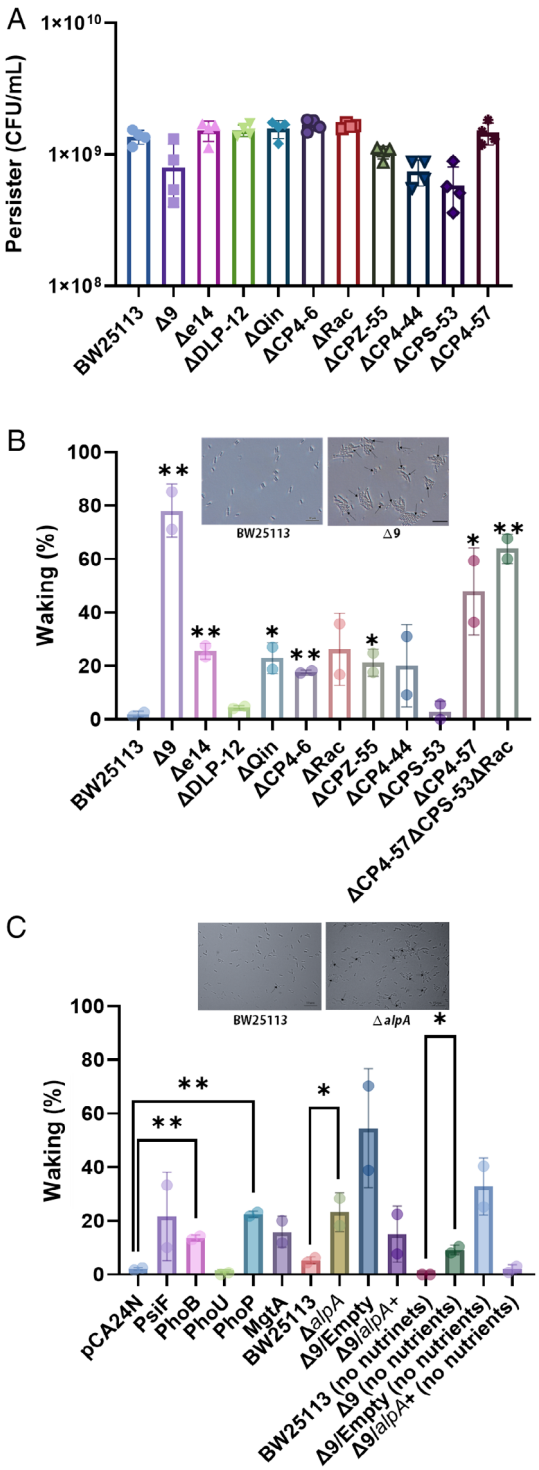

Fig. 1. Cryptic prophages have no effect on persister cell formation but reduce single-cell persister resuscitation by repressing phosphate sensing.

A. Cryptic prophages do not affect persister cell formation. Persister cell formation (CFU ml^{-1}) was determined by cell counts on LB plates after 1 day. These results are the average of four independent cultures and error bars indicate standard deviations.

B. Cryptic prophages reduce persister cell resuscitation. Single-cell persister resuscitation after 4 h at 37°C with 0.4 wt.% glucose as

Fig. 1. Legend on next column.

ampicillin (Kwan *et al*., 2013). Hence, although cryptic prophages dramatically increase resistance to stresses (Wang *et al*., 2010), they do not change the number of the cells that become persisters. These results are similar to those of .Harms *et al*., (2017) who utilized our Δ9 strain (Wang *et al*., 2010) and found little impact on the number of persister cells after treating with ciprofloxacin.

Cryptic prophages reduce persister resuscitation

To investigate further the role of cryptic prophages in persistence, we quantified single cell resuscitation for the Δ9 strain in the M9 glucose medium. In stark contrast to the lack of impact of the cryptic prophages on persister cell *formation* (Fig. 1A), deleting the nine cryptic prophages dramatically increased persister cell *resuscitation* (44-fold, Fig. 1B, Fig. S1, Table S2). The criteria for resuscitation are elongation, appearance of a septum, or increase in cell number, and movies have been published previously for resuscitating cells using our approach (Kim *et al*., 2018a; Kim *et al*., 2018b). Also, extending the resuscitation time by 50% did not change the number of waking cells.

Remarkably, nearly all of the persister cells that lack cryptic prophage (80%) were resuscitated within 4 h compared to 2% of the wild-type strain. Similar results were obtained by treating only with ampicillin to form persister cells (i.e. foregoing rifampicin pre-treatment, Fig. S2) in that 66% of the single cells resuscitated in the absence of the cryptic prophages (a 34-fold increase). Further corroboration of the results with the Δ9 strain (166 kb deleted) came by testing for single-cell resuscitation of *E. coli* MDS66 (Karcagi *et al*., 2016) which has 19% of the

determined using light microscopy for each of the single cryptic prophage deletions as well as for the Δ9 strain. Representative results from two independent cultures are shown, tabulated cell numbers are shown in Table S2, and representative images are shown in Fig. S1. Representative images for BW25113 and Δ9 resuscitating shown in the inset.

C. PhoB increases single-cell persister resuscitation. Single-cell persister resuscitation after 6 h for BW25113/pCA24N versus BW25113/pCA24N_*psiF* ('PsiF'), BW25113/pCA24N versus BW25113/pCA24N_*phoB* ('PhoB') and BW25113/pCA24N versus BW25113/pCA24N_*phoU* ('PhoU'), after 4 h for BW25113 versus BW25113 Δ*alpA*, after 3 h for Δ9/pCA24N versus Δ9/pCA24N_*alpA*, and after 3 h for BW25113 (no nutrients) versus BW25113 Δ9 (no nutrients); the different resuscitation times were used to distinguish more clearly the differences in resuscitation. Cells were resuscitated at 37°C with 0.4 wt.% glucose (except for the 'no nutrient' group) as determined using light microscopy. Representative results from two independent cultures are shown, tabulated cell numbers are shown in Table S3, and representative images are shown in Fig. S4. Representative images for BW25113 and Δ*alpA* resuscitating shown as the inset. Student's *t*-tests were used to compare pairs (asterisk indicates a *p*-value <0.05 and double asterisk indicates a *p*-value <0.01). [Color figure can be viewed at wileyonlinelibrary.com]

© 2021 Society for Applied Microbiology and John Wiley & Sons Ltd., *Environmental Microbiology*

chromosome deleted (891 kb) including the cryptic prophages deleted; this strain also had a 17-fold higher resuscitation than the wild-type (Fig. S3; Table S2). Also, the phenotype is restricted to persister resuscitation since re-growth from the stationary phase (turbidity 6) was not affected for the Δ9 strain relative to the wild-type strain.

The impact of each cryptic prophage was tested using each of the single complete prophage deletions (Wang *et al*., 2010), and the frequency of waking was increased by 2.3- to 25-fold (Figs 1B and S1; Table S2); the frequency of resuscitation was greatest upon deleting the genes of cryptic phage CP4-57 (25-fold). Since ΔCP4-57 has the largest effect, we also tested a triple knockout (ΔCPS-53 ΔCP4-57 ΔRac) with this strain and, as expected, found resuscitation increased 32-fold respectively. Hence, each cryptic prophage reduces the frequency of persister cell resuscitation although the contribution of each varies.

Cryptic prophages repress resuscitation by reducing phosphate sensing

To elucidate the mechanism by which the cryptic prophages reduce persister cell resuscitation, a whole-transcriptome analysis of resuscitating persister cells for Δ9 was compared to the wild-type under the same conditions (Table 1). Remarkably, transcription of eight tRNA genes was induced dramatically, which confirms the importance of the initiation of translation for resuscitating cells (Kim *et al*., 2018b; Song and Wood, 2020a, 2020b; Yamasaki *et al*., 2020). Furthermore, *ssrA* was induced, which serves as a positive control since ribosome recovery via SsrA has been shown to facilitate persister cell resuscitation (Yamasaki *et al*., 2020) (Table 1). Also, the chaperones DnaK, GroS and IbpA, from the upregulated genes in the resuscitating cells here, have been linked with persister cell resuscitation, too (Bollen *et al*., 2021; Dewachter *et al*., 2021), so they also serve as positive controls. Similar to the tRNA and chaperone genes, phosphate/Mg^{+2}/Mn^{+2}-sensing/transport genes *pstSCB*, *phoB*, *psiF*, *mgtL*, *mgtS* and *mntS* were induced in the absence of the cryptic prophages. PhoR-PhoB comprise a two-component regulatory system that activates the phosphate-specific transport (Pst) system that includes the outer membrane ATP-binding cassette proteins PstSCAB, which act as an inorganic phosphate sensor (Kritmetapak and Kumar, 2021), and MgtA-MgtS regulate the PitAB low-affinity phosphate transport to increase phosphate when Mg^{+2} is limiting and stimulate PhoB (Yin *et al*., 2019). Therefore, the whole-transcriptome data suggest deletion of the cryptic prophages increases persister resuscitation by increasing phosphate sensing.

Phosphate transport increases persister cell resuscitation

Since the phosphate transport locus *pstSCAB* is activated by the response regulator PhoB, which in turn, is activated by the kinase activity of PhoR (Santos-Beneit, 2015) (Fig. 2), we hypothesized that the cryptic prophages contain at least one negative regulator that represses either *phoR* or *phoB*. Hence, activation of PhoR or PhoB should increase persister resuscitation.

To test this hypothesis, PhoB was produced from pCA24N-*phoB* in phosphate-replete conditions (i.e. using M9 buffer with 0.4% glucose) so that any effect would be under conditions where the phosphate transport system is normally repressed. Under these conditions, persister resuscitation was increased eightfold by producing PhoB compared to the empty plasmid (Figs 1C and S4; Table S3). Furthermore, production of PhoU, the negative regulator of PhoR, via pCA24N-*phoU*, reduced resuscitation by fourfold (Figs 1C and S4; Table S3), as expected. Note that the phosphate starvation protein PsiF, which is positively regulated by PhoB, was previously shown to increase persister resuscitation sixfold when produced from pCA24N-*psiF* (Yamasaki *et al*., 2020).

In addition, since cAMP reduces persister resuscitation (Yamasaki *et al*., 2020), we tested cAMP levels upon producing PhoB and found cAMP levels are reduced -3.8 ± 0.2-fold. Given that PhoB represses *cra* transcription (Marzan and Shimizu, 2011; Marzan *et al*., 2013) and that Cra increases cAMP (Crasnier-Mednansky *et al*., 1997), we tested whether the *cra* mutation reduces cAMP and found a 27 ± 5% decrease in cAMP. Furthermore, production of PhoB via pCA24N_*phoB* increased *pstB* transcription by 7 ± 2-fold.

Since phosphate transport by PitAB leads to activation of PhoP and MgtA/MgtS, which serves to activate PhoB (Yin *et al*., 2019), we tested whether production of PhoP and MgtA increase resuscitation. As expected, resuscitation was increased 11-fold and 8-fold respectively (Figs 1C and S4; Table S3). Hence, activation of the phosphate sensing system increases resuscitation through PhoB, PsiF, PhoP and MgtA, and negative regulator PhoU reduces resuscitation.

AlpA from cryptic prophage CP4-57 represses phosphate sensing

To investigate how the cryptic prophages reduce resuscitation through phosphate sensing, the impact of deleting three DNA putative regulators, *yfjR*, *alpA*, and *yfjP*, from cryptic prophage CP4-57, was evaluated, since this cryptic prophage had the largest impact on persister cell resuscitation. It seemed reasonable to suppose these regulators could possibly directly or indirectly influence phosphate

© 2021 Society for Applied Microbiology and John Wiley & Sons Ltd.,

Table 1. Most-induced genes during persister cell resuscitation for BW25113 Δ9 versus BW25113.

Gene	Description	Fold Change	Pi Activated
Ribosomes			
ssrA	Transfer-messenger RNA to recover ribosomes	5.2	
thrW	tRNA-Thr	∞	
leuW	tRNA-Leu	∞	
glyU	tRNA-Gly	∞	
argX	tRNA-Arg	∞	
thrT	tRNA-Thr	∞	
leuX	tRNA-Leu	∞	
hisR	tRNA-His	5.2	
serU	tRNA-Ser	3.3	
Stress response			
rprA	Small regulator	∞	Yes
yqgB	Acid stress response protein	∞	
rhsC	rhs element protein RhsC	4.8	
P_i and metal Transport/homeostasis			
mgtL	Leader peptide for *mgtA* in response to magnesium ion levels	∞	Yes
mgtS	Mg^{2+} transporter, with MgtA, activates PitAB for low-affinity phosphate/Mg^{2+} accumulation	4.2	Yes
chaB	Putative cation transport regulator ChaB	3.6	
mntS	Manganese accumulation protein MntS	3.2	
pstB	Phosphate ABC transporter ATP-binding protein	1.8	Yes
pstC	Phosphate ABC transporter permease	1.4	Yes
pstS	Phosphate ABC transporter substrate-binding protein	1.6	Yes
phoB	Phosphate transcriptional regulator	1.6	Yes
psiF	Phosphate starvation-inducible protein	1.2	Yes
Chaperones			
paoD	Molybdenum cofactor insertion chaperone	1.8	
groS	Co-chaperone GroES	4.5	
ibpA	Heat shock chaperone IbpA	3.5	
dnaK	Molecular chaperone DnaK	3.3	
Others			
envy	DNA-binding transcriptional regulator	3.4	
ilvL	ilvXGMEDA operon leader peptide	13.0	
icd	Isocitrate dehydrogenase	10.8	Yes
cydX	Cytochrome bd-I oxidase subunit CydX	4.6	
ytjA	DUF1328 domain-containing protein	3.8	
ymiA	Uncharacterized protein YmiA	3.7	
cysI	Assimilatory sulfite reductase hemoprotein subunit	1.6	

Persister cells were formed using the rifampicin/ampicillin method, and persister cells were resuscitated by adding M9 glucose (0.4 wt.%) for 10 min (i.e. phosphate-replete conditions). Two independent cultures were used for each strain. Complete results are in Excel File S1 and a heat map for 175 genes is shown in Supplemental Fig. 5.

import. On agar plates, the *alpA* mutant woke faster than *yfjR* and *yfjP* as evidenced by consistently larger colonies; hence, we focused on the *alpA* mutant. Using single-cell microscopy and six independent cultures, the *alpA* deletion consistently increased persister cell resuscitation by 4.4-fold (Figs 1C and S4; Table S3); hence, AlpA of cryptic prophage CP4-57 reduces persister resuscitation. Moreover, production of AlpA from pCA24N complemented the *alpA* deletion by reducing persister resuscitation 4.1-fold (Figs 1C and S4; Table S3). Strikingly, rather than being a metabolic burden, production of AlpA *increased* the specific growth fourfold in rich medium; hence, AlpA has a large impact on metabolism.

To explore how AlpA influences phosphate import, qRT-PCR was used to investigate AlpA activation of *phoR*, *phoB* and *pstB* in the absence of the nine cryptic prophages. Compared to the empty plasmid, production of AlpA via pCA24N-*alpA* in the Δ9 strain repressed *phoB*, *phoR* and *pstB* (Table S4); hence, AlpA likely binds to the *phoB* promoter resulting in the repression of the downstream phosphate-sensing proteins PhoR and PstB (Fig. 2).

Δ9 persisters resuscitate without a carbon source

Given the cryptic prophages repress resuscitation by reducing phosphate sensing, perhaps the role of the phage fossils was to prevent persister cell resuscitation in the absence of a carbon source, since PhoB is a master regulator; for example, the starvation response via ppGpp activates the Pho regulon (Santos-Beneit, 2015). Therefore, testing for persister cell resuscitation in the absence of glucose but in the presence of phosphate (i.e. M9 medium that lacks nutrients), the Δ9 strain resuscitates without glucose (9 ± 2%, Figs 1C and S4;

© 2021 Society for Applied Microbiology and John Wiley & Sons Ltd., *Environmental Microbiology*

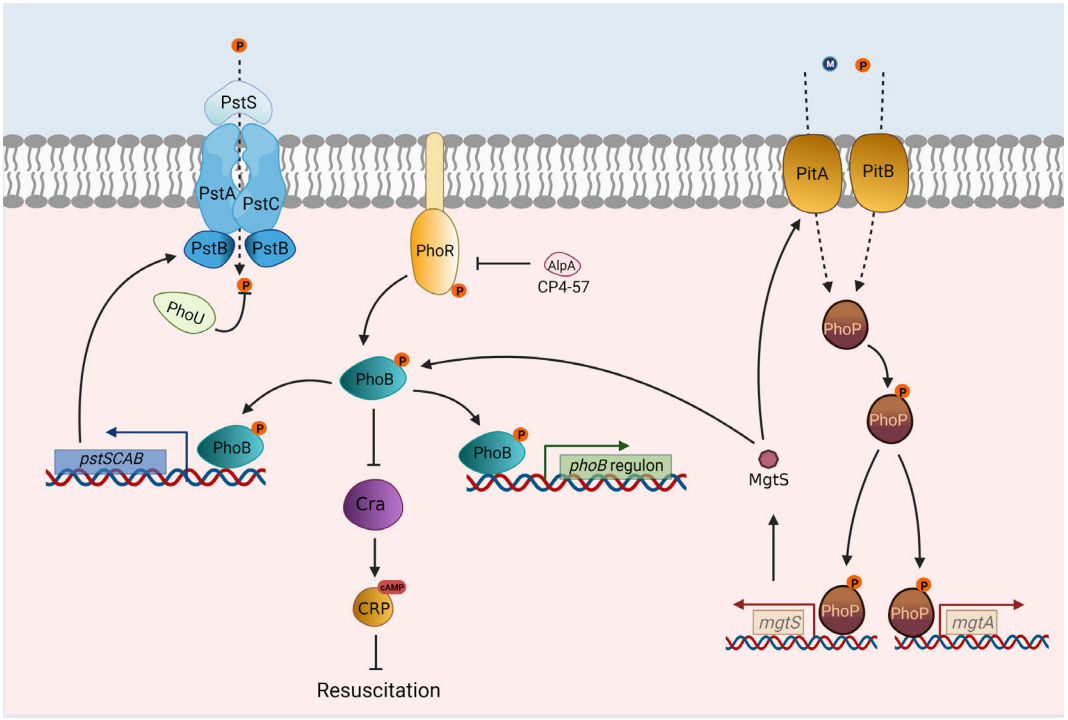

Fig. 2. Schematic of the impact of phosphate sensing and cryptic prophage AlpA on persister cell resuscitation. AlpA (from cryptic prophage CP4-57) likely represses *phoR* that encodes the phosphate-dependent PhoR/PhoB two-component signal transduction system. PhoR/PhoB sense external phosphate and are active when concentrations of external phosphate are low. PhoR phosphorylates PhoB which induces the *pstSCAB* operon and facilitates phosphate uptake. PhoP is also activated by phosphate transport through the PitAB system, and phosphorylated PhoP induces small protein MgtS, which activates PhoB. PhoB increases persister cell resuscitation by reducing cAMP by silencing *cra* transcription. Ⓟ indicates phosphate, → indicates induction and ⊥ indicates repression. This figure was created with BioRender.com. [Color figure can be viewed at wileyonlinelibrary.com]

Table S3), whereas the wild-type strain cannot resuscitate without glucose, as was found previously for the absence of LB medium (Kim *et al*., 2018b) and alanine (Yamasaki *et al*., 2020). Note this increased waking by Δ9 is even more surprising since Δ9 grows slightly slower than wild-type (1.36 ± 0.01 vs. 1.46 ± 0.02 h^{-1} in rich medium for Δ9 and the wild-type strain respectively) (Wang *et al*., 2010). Furthermore, this phenotype was complemented by producing AlpA in the Δ9 strain (Figs 1C and S4, Table S3). Hence, the cryptic prophages, through at least AlpA, prevent premature persister resuscitation.

Discussion

As an interwoven means of cell regulation, our results show that cryptic prophages not only help the cell respond to stress as an active response (Wang *et al*., 2010) but also regulate the exit of the cell from dormancy. Specifically, cryptic prophages control persister cell resuscitation through their inhibition of phosphate sensing, as revealed by the use of transcriptomics for resuscitating persister cells. Clearly, although each of the nine cryptic prophages consistently inhibit persister resuscitation, cryptic prophage CP4-57 has the greatest effect (Fig. 1B), and regulator AlpA of CP4-57 was shown here to inhibit persister resuscitation. Although there was a 44-fold increase in waking with Δ9 and only a 4.4-fold increase with Δ*alpA*, there must be additional cryptic prophage proteins used by the host to reduce persister resuscitation. This is reasonable given that each of the nine cryptic prophages impacted resuscitation.

The mechanism for AlpA reducing resuscitation is likely by AlpA repressing *phoR*; *phoR* encodes the membrane-bound, sensor histidine kinase regulator of the phosphate-dependent PhoR/PhoB two-component signal transduction system that senses external phosphate (Fig. 2); PhoR/PhoB are active when concentrations of external phosphate are low (Kritmetapak and Kumar, 2021) by PhoR phosphorylating PhoB which induces the *pstSCAB* operon and facilitates phosphate uptake (Santos-Beneit, 2015). AlpA is a poorly characterized, small (70 aa) regulator that likely binds DNA due to its helix-turn-helix DNA-binding motif (Keseler *et al*., 2017); note the primary sequence only contains the DNA-binding motif due to its small size. AlpA is active

© 2021 Society for Applied Microbiology and John Wiley & Sons Ltd., *Environmental Microbiology*

in *E. coli* since it has been linked to AI-2 quorum-sensing in this strain [*alpA* is induced upon inactivation of the AI-2 exporter TqsA (Herzberg *et al*., 2006)], and *alpA* is induced in *E. coli* mature biofilms (Domka *et al*., 2007). Moreover, AlpA is a known transcriptional regulator since it causes excision of CP4-57 (Wang *et al*., 2009) by inducing *intA* (Kirby *et al*., 1994). Therefore, in the absence of AlpA, due to deleting cryptic prophage CP-457, derepression of *phoR* occurs, and we hypothesize that PhoR stimulates PhoB through phosphorylation, and phosphorylated PhoB increases persister cell resuscitation by reducing cAMP by silencing *cra* transcription (Marzan and Shimizu, 2011; Marzan *et al*., 2013), since Cra increases cAMP (Crasnier-Mednansky *et al*., 1997). Decreasing cAMP was shown to dramatically increase resuscitation (Yamasaki *et al*., 2020), and we found here that PhoB reduces cAMP and that *cra* reduced cAMP (summarized in Fig. 2).

Phosphate has been linked previously to persister cells formation, but, phosphate has not been studied previously for its impact on persister cell resuscitation. For *E. coli* persister cell formation, the phosphate regulator PhoU has been identified as a positive effector for persister cell formation (Li and Zhang, 2007). However, the mechanism by which PhoU controls *E. coli* persister cell formation was not determined (Namugenyi *et al*., 2017), although, in *S. aureus*, *phoU* deletion appears to reduce persistence by increasing slightly carbon metabolism (Shang *et al*., 2020). PhoU regulates phosphate transport by repressing the Pst system at high phosphate concentrations (Namugenyi *et al*., 2017). In addition, the *Mycobacterium tuberculosis* PhoU orthologues PhoY1 and PhoY2 also increase persister cell formation (Namugenyi *et al*., 2017). Therefore, these results on the cryptic prophages of *E. coli* reducing persister cell resuscitation fit well with these previous persister cell formation results related to phosphate since PhoU negatively regulates *phoR*/*phoB* (Kritmetapak and Kumar, 2021) (Fig. 2); i.e. PhoU increases persister cell *formation* (Li and Zhang, 2007; Namugenyi *et al*., 2017), and here PhoB stimulates persister cell *resuscitation*. Moreover, these results suggest a mechanism for the previous results indicating the negative regulator PhoU increases persistence: PhoU likely increases persistence by increasing cAMP through its inhibition of PhoB (Fig. 2). In addition, we also found that the transcriptional regulator PhoP, which leads to PhoB activation through the small protein regulator MgtS (Yin *et al*., 2019), increases resuscitation and this fits well with recent results showing PhoP is important for the recovery of *Salmonella enterica* from magnesium starvation (Yeom and Groisman, 2021).

The physiological benefit of reducing persister resuscitation appears to be to allow the cell to monitor more than phosphate concentrations before committing resources to waking. By deleting the cryptic prophages and negative regulators like AlpA, this highly regulated return to active metabolism is short-circuited, leading to the dramatic increase seen in resuscitation, even in the absence of nutrients. Clearly, with limited ATP, the cell must optimize resuscitation (e.g. unlike exponentially growing cells, persisters cannot wake without a carbon source in the presence of the cryptic prophages [Kim *et al*., 2018b; Yamasaki *et al*., 2020)]; hence, these results suggest the cell monitors the availability of carbon along with phosphate, before committing to resuscitation. Moreover, they add credence to the idea that persister resuscitation is elegantly regulated (Yamasaki *et al*., 2020).

Materials and methods

Bacteria and growth conditions

Bacteria (Table S5; Baba *et al*., 2006; Kitagawa *et al*., 2005) were cultured routinely in lysogeny broth (Bertani, 1951) at 37°C. The Δ9 strain lacking all nine *E. coli* cryptic prophage genes (Wang *et al*., 2010) was verified previously through DNA microarrays to confirm that there were no undesired deletions and that each of the nine cryptic prophages was deleted completely (Wang *et al*., 2010); the RNA-seq work here also corroborated this. There was no difference in minimum inhibitory concentrations (Kwan *et al*., 2013) for the wild-type and Δ9 strain with ampicillin and rifampicin. The single cryptic prophage strains were verified by DNA sequencing (Wang *et al*., 2010). The pCA24N-based plasmids (Kitagawa *et al*., 2005) were retained in overnight cultures via chloramphenicol (30 μg ml^{-1}), and kanamycin (50 μg/ml^{-1}) was used for deletion mutants, where applicable. M9 glucose (0.4 wt.%) medium (Rodriguez and Tait, 1983) (M9-Glu) was used for persister cell resuscitation.

Persister cells

Exponentially growing cells (turbidity of 0.8 at 600 nm) were converted to persister cells (Kwan *et al*., 2013; Kim *et al*., 2018b) by adding rifampicin (100 μg ml^{-1}) for 30 min to stop transcription, centrifuging and adding LB with ampicillin (100 μg ml^{-1}) for 3 h to lyse non-persister cells. To remove ampicillin, cells were washed twice with 0.85% NaCl then re-suspended in 0.85% NaCl. Persister concentrations were enumerated via a drop assay (Donegan *et al*., 1991).

ATP assay

To measure ATP concentrations in persister cells and in resuscitating cells, persister cells were formed with

© 2021 Society for Applied Microbiology and John Wiley & Sons Ltd., *Environmental Microbiology*

rifampicin/ampicillin treatment as indicated above and for resuscitating cells, persister cells were resuspended in M9-Glu medium for 10 min. Samples (1 ml) were washed once and resuspended in Tris-acetate buffer (50 mM, pH 7.75), then the ATP assay was performed in duplicate using the ENLTEN ATP Assay System (Promega, cat#: FF2000) with the luminescence measured via a Turner Design 20E Luminometer using a 5 s time delay and a 10 s integration time.

Single-cell persister resuscitation

Persister cells (5 μl) were added to 1.5% agarose gel pads containing M9-Glu medium, and single-cell resuscitation was visualized at 37°C via a light microscope (Zeiss Axio Scope.A1, bl_ph channel at 1000 ms exposure). For each condition, at least two independent cultures were used with 150–300 individual cells used per culture.

RNA-Seq

To elucidate the transcriptome differences upon resuscitation of the Δ9 strain versus wild-type, both strains were grown to a turbidity of 0.8 at 600 nm and converted into populations that solely consist of persisters by rifampicin and ampicillin treatment as indicated above, and resuscitated for 10 min in M9-Glu medium. Samples for RNA were added to cold 1.9 ml tubes containing RNA-Later, quick-cooled in dry ice 95% ethanol, centrifuged, and the cell pellets were frozen at −80°C. RNA was harvested using the High Pure RNA Isolation Kit (Roche, Basel, Switzerland). Two independent samples were analysed. The resultant library of RNA samples was quantified by a Bioanalyzer (Agilant) and sequenced by Illumina HiSeq 4000. Low-quality reads and adapter sequences were filtered by cutadapt v2.8 [quality-cutoff (20), minimum-length (50)] (Martin, 2011). Filtered reads were mapped to the reference genome (NZ_CP009273.1) using STAR v2.7.1a followed by ENCODE standard parameters (Dobin *et al*., 2013). Using the read mapping information obtained using the aligner, the expression levels of genes and transcripts were calculated using featureCounts v2.0.0, Cufflinks v2.2.1 (multi-read-correct, frag-bias-correct) (Trapnell *et al*., 2010; Liao *et al*., 2014). Differential expressed genes were calculated by DESeq2 v1.26.0 (Love *et al*., 2014). Genes were identified as differentially expressed if the *p*-value was less than 0.05 and if the expression ratio was greater than the standard deviation for all the genes (0.5). As expected, about 240 cryptic prophage genes yielded no signal for the Δ9 strain (Excel file S1).

qRT-PCR

To investigate the impact of AlpA production on phosphate sensing, qRT-PCR was performed for the phosphate sensing regulators *phoR*, *phoB* and *pstB* by producing AlpA from pCA24N-*alpA* in host Δ9 (compared to Δ9/pCA24N) that lacks AlpA in the chromosome. Cells were grown in LB until a turbidity of 0.4 at 600 nm, then *alpA* was induced with isopropyl β-D-1-thiogalactopyranoside (1 mM) for 90 min. RNA was isolated as for RNA-seq (above), *purM* was used as the housekeeping gene and qRT-PCR was performed using Power SYBR Green RNA-to-CT 1-Step with a CFX96 Real-Time System and 100 ng of RNA along with the primers shown in Table S6.

cAMP

cAMP levels were assayed using the non-acetylated format of the ENZO ELISA Kit (ADI-900-067). Cells were grown in LB to a turbidity of 0.8 at 600 nm (for the *cra* mutant) or to a turbidity of 0.3, followed by protein production via induction with 0.5 mM IPTG for 1 h (for BW25113/pCA24N_*phoB*), then lysed.

Acknowledgements

This work was supported by funds derived from the Biotechnology Endowed Professorship at the Pennsylvania State University for T.K.W., from the National Research Foundation of Korea (NRF) grant from the Korean Government (NRF-2020R1F1A1072397) for S.S. and from the National Research Foundation of Korea (NRF) funded by the Korean government (MSIT) (NRF-2019R1C1C1008856) for J.-S.K.

References

Baba, T., Ara, T., Hasegawa, M., Takai, Y., Okumura, Y., Baba, M., *et al*. (2006) Construction of *Escherichia coli* K-12 in-frame, single-gene knockout mutants: the Keio collection. *Mol Syst Biol* **2**: 0008.

Bertani, G. (1951) Studies on Lysogenesis. 1. The mode of phage liberation by lysogenic *Escherichia coli*. *J Bacteriol* **62**: 293–300.

Bollen, C., Dewachter, L., and Michiels, J. (2021) Protein aggregation as a bacterial strategy to survive antibiotic treatment. *Front Molec Biosci* **8**: v669664.

Casjens, S. (2003) Prophages and bacterial genomics: what have we learned so far? *Mol Microbiol* **49**: 277–300.

Chowdhury, N., Kwan, B.W., and Wood, T.K. (2016) Persistence increases in the absence of the alarmone guanosine tetraphosphate by reducing cell growth. *Sci Rep* **6**: 20519.

Crasnier-Mednansky, M., Park, M.C., Studley, W.K., and Saier, M.H. (1997) Cra-mediated regulation of *Escherichia coli* adenylate cyclase. *Microbiology* **143**: 785–792.

Cui, P., Niu, H., Shi, W., Zhang, S., Zhang, W., and Zhang, Y. (2018) Identification of genes involved in bacteriostatic antibiotic-induced persister formation. *Front Microbiol* **9**: 413.

© 2021 Society for Applied Microbiology and John Wiley & Sons Ltd.,

Dewachter, L., Bollen, C., Wilmaerts, D., Louwagie, E., Herpels, P., Matthay, P., *et al*. (2021) The dynamic transition of persistence toward the viable but Nonculturable state during stationary phase is driven by protein aggregation. *mBio* **12**: e00703-00721.

Dobin, A., Davis, C.A., Schlesinger, F., Drenkow, J., Zaleski, C., Jha, S., *et al*. (2013) STAR: ultrafast universal RNA-seq aligner. *Bioinformatics* **29**: 15–21.

Domka, J., Lee, J., Bansal, T., and Wood, T.K. (2007) Temporal gene-expression in *Escherichia coli* K-12 biofilms. *Environ Microbiol* **9**: 332–346.

Donegan, K., Matyac, C., Seidler, R., and Porteous, A. (1991) Evaluation of methods for sampling, recovery, and enumeration of bacteria applied to the phylloplane. *Appl Environ Microbiol* **57**: 51–56.

Goormaghtigh, F., Fraikin, N., Putrinš, M., Hallaert, T., Hauryliuk, V., Garcia-Pino, A., *et al*. (2018) Reassessing the role of type II toxin-antitoxin Systems in Formation of *Escherichia coli* type II Persister cells. *mBio* **9**: e00640-00618.

Goormaghtigh, F., and Van Melderen, L. (2019) Single-cell imaging and characterization of *Escherichia coli* persister cells to ofloxacin in exponential cultures. *Sci Adv* **5**: eaav9462.

Grassi, L., Di Luca, M., Maisetta, G., Rinaldi, A.C., Esin, S., Trampuz, A., and Batoni, G. (2017) Generation of Persister cells of *Pseudomonas aeruginosa* and *Staphylococcus aureus* by chemical treatment and evaluation of their susceptibility to membrane-targeting agents. *Front Microbiol* **8**: 1917.

Harms, A., Fino, C., Sørensen, M.A., Semsey, S., and Gerdes, K. (2017) Prophages and growth dynamics confound experimental results with antibiotic-tolerant persister cells. *mBio* **8**: e01964-01917.

Herzberg, M., Kaye, I.K., Peti, W., and Wood, T.K. (2006) YdgG (TqsA) controls biofilm formation in *Escherichia coli* K-12 by enhancing autoinducer 2 transport. *J Bacteriol* **188**: 587–598.

Hong, S.H., Wang, X., O'Connor, H.F., Benedik, M.J., and Wood, T.K. (2012) Bacterial persistence increases as environmental fitness decreases. *Microbial Biotechnol* **5**: 509–522.

Jin, X., Kightlinger, W., Kwon, Y.-C., and Hong, S.H. (2018) Rapid production and characterization of antimicrobial colicins using *Escherichia coli*-based cell-free protein synthesis. *Syn Biol* **3**: ysy004.

Johnson, P.J.T., and Levin, B.R. (2013) Pharmacodynamics, population dynamics, and the evolution of persistence in *Staphylococcus aureus*. *PLOS Gen* **9**: e1003123.

Karcagi, I., Draskovits, G., Umenhoffer, K., Fekete, G., Kovács, K., Méhi, O., *et al*. (2016) Indispensability of horizontally transferred genes and its impact on bacterial genome streamlining. *Molec Biol Evol* **33**: 1257–1269.

Keseler, I.M., Mackie, A., Santos-Zavaleta, A., Billington, R., Bonavides-Martínez, C., Caspi, R., *et al*. (2017) The EcoCyc database: reflecting new knowledge about *Escherichia coli* K-12. *Nucl Acids Res* **45**, D543–D550.

Kim, J.-S., Chowdhury, N., Yamasaki, R., and Wood, T.K. (2018a) Viable but non-Culturable and persistence describe the same bacterial stress state. *Environ Microbiol* **20**: 2038–2048.

Kim, J.-S., Yamasaki, R., Song, S., Zhang, W., and Wood, T.K. (2018b) Single cell observations show Persister cells wake based on ribosome content. *Environ Microbiol* **20**: 2085–2098.

Kirby, J.E., Trempy, J.E., and Gottesman, S. (1994) Excision of a P4-like cryptic prophage leads to alp protease expression in Escherichia coli. *J Bacteriol* **176**: 2068–2081.

Kitagawa, M., Ara, T., Arifuzzaman, M., Ioka-Nakamichi, T., Inamoto, E., Toyonaga, H., and Mori, H. (2005) Complete set of ORF clones of *Escherichia coli* ASKA library (a complete set of *E. coli* K-12 ORF archive): unique resources for biological research. *DNA Res* **12**: 291–299.

Korch, S.B., Henderson, T.A., and Hill, T.M. (2003) Characterization of the *hipA7* allele of *Escherichia coli* and evidence that high persistence is governed by (p)ppGpp synthesis. *Mol Microbiol* **50**: 1199–1213.

Kritmetapak, K., and Kumar, R. (2021) Phosphate as a signaling molecule. *Calcif Tissue Int* **108**: 16–31.

Kwan, B.W., Valenta, J.A., Benedik, M.J., and Wood, T.K. (2013) Arrested protein synthesis increases persister-like cell formation. *Antimicrob Agents Chemother* **57**: 1468–1473.

Lewis, K. (2008) Multidrug tolerance of biofilms and persister cells. *Curr Top Microbiol Immunol* **322**: 107–131.

Li, Y., and Zhang, Y. (2007) PhoU is a persistence switch involved in persister formation and tolerance to multiple antibiotics and stresses in *Escherichia coli*. *Antimicrob Agents Chemother* **51**: 2092–2099.

Liao, Y., Smyth, G.K., and Shi, W. (2014) featureCounts: an efficient general purpose program for assigning sequence reads to genomic features. *Bioinformatics* **30**: 923–930.

Love, M.I., Huber, W., and Anders, S. (2014) Moderated estimation of fold change and dispersion for RNA-seq data with DESeq2. *Gen Biol* **15**: 550.

Martin, M. (2011) Cutadapt removes adapter sequences from high-throughput sequencing reads. *EMBnetjournal* **17**: 1.

Martins, D., McKay, G.A., English, A.M., and Nguyen, D. (2020) Sublethal Paraquat confers multidrug tolerance in *Pseudomonas aeruginosa* by inducing superoxide dismutase activity and lowering envelope permeability. *Front Microbiol* **11**: 576708.

Marzan, L.W., Hasan, C.M.M., and Shimizu, K. (2013) Effect of acidic condition on the metabolic regulation of *Escherichia coli* and its *phoB* mutant. *Arch Microbiol* **195**: 161–171.

Marzan, L.W., and Shimizu, K. (2011) Metabolic regulation of Escherichia coli and its phoB and phoR genes knockout mutants under phosphate and nitrogen limitations as well as at acidic condition. *Microb Cell Factor* **10**: 39.

Mohiuddin, S.G., Kavousi, P., and Orman, M.A. (2020) Flow-cytometry analysis reveals persister resuscitation characteristics. *BMC Microbiol* **20**: 202.

Namugenyi, S.B., Aagesen, A.M., Elliott, S.R., and Tischler, A.D. (2017) *Mycobacterium tuberculosis* PhoY proteins promote Persister formation by mediating Pst/-SenX3-RegX3 phosphate sensing. *mBio* **8**: e00494-00417.

Narayanaswamy, V.P., Keagy, L.L., Duris, K., Wiesmann, W., Loughran, A.J., Townsend, S.M., and Baker, S. (2018) Novel glycopolymer eradicates antibiotic-

© 2021 Society for Applied Microbiology and John Wiley & Sons Ltd., *Environmental Microbiology*

and CCCP-induced persister cells in *Pseudomonas aeruginosa*. *Front Microbiol* **9**: 1724.
Nguyen, D., Joshi-Datar, A., Lepine, F., Bauerle, E., Olakanmi, O., Beer, K., *et al*. (2011) Active starvation responses mediate antibiotic tolerance in biofilms and nutrient-limited bacteria. *Science* **334**: 982–986.
Pu, Y., Li, Y., Jin, X., Tian, T., Ma, Q., Zhao, Z., *et al*. (2019) ATP-dependent dynamic protein aggregation regulates bacterial dormancy depth critical for antibiotic tolerance. *Mol Cell* **73**: 143–156.
Rodriguez, R.L., and Tait, R.C. (1983) *Recombinant DNA Techniques: An Introduction*. Menlo Park, CA: Benjamin/Cummings Publishing.
Rowe, S.E., Wagner, N.J., Li, L., Beam, J.E., Wilkinson, A. D., Radlinski, L.C., *et al*. (2020) Reactive oxygen species induce antibiotic tolerance during systemic *Staphylococcus aureus* infection. *Nat Microbiol* **5**: 282–290.
Santos-Beneit, F. (2015) The pho regulon: a huge regulatory network in bacteria. *Front Microbiol* **6**: 402.
Shang, Y., Wang, X., Chen, Z., Lyu, Z., Lin, Z., Zheng, J., *et al*. (2020) *Staphylococcus aureus* PhoU homologs regulate Persister formation and virulence. *Front Microbiol* **11**: 865.
Shimada, T., Yoshida, H., and Ishihama, A. (2013) Involvement of cyclic AMP receptor protein in regulation of the *rmf* gene encoding the ribosome modulation factor in *Escherichia coli*. *J Bacteriol* **195**: 2212–2219.
Song, S., and Wood, T.K. (2018) Post-segregational killing and phage inhibition are not mediated by cell death through toxin/antitoxin systems. *Front Microbiol* **9**: 814.
Song, S., and Wood, T.K. (2020a) ppGpp ribosome dimerization model for bacterial persister formation and resuscitation. *Biochem Biophys Res Commun* **523**: 281–286.
Song, S., and Wood, T.K. (2020b) Persister cells resuscitate via ribosome modification by 23S rRNA Pseudouridine synthase RluD. *Environ Microbiol* **22**: 850–857.
Sulaiman, J.E., Hao, C., and Lam, H. (2018) Specific enrichment and proteomics analysis of *Escherichia coli* Persisters from rifampin pretreatment. *J Proteome Res* **17**: 3984–3996.
Sun, F., Bian, M., Li, Z., Lv, B., Gao, Y., Wang, Y., and Fu, X. (2020) 5-Methylindole potentiates aminoglycoside against gram-positive bacteria including *Staphylococcus aureus* persisters under hypoionic conditions. *Front Cell Infect Microbiol* **10**: 84.
Svenningsen, M.S., Veress, A., Harms, A., Mitarai, N., and Semsey, S. (2019) Birth and resuscitation of (p)ppGpp induced antibiotic tolerant persister cells. *Sci Rep* **9**: 6056.
Tkhilaishvili, T., Lombardi, L., Klatt, A.-B., Trampuz, A., and Di Luca, M. (2018) Bacteriophage Sb-1 enhances antibiotic activity against biofilm, degrades exopolysaccharide matrix and targets persisters of *Staphylococcus aureus*. *Int J Antimicrob Agents* **52**: 842–853.
Trapnell, C., Williams, B.A., Pertea, G., Mortazavi, A., Kwan, G., van Baren, M.J., *et al*. (2010) Transcript assembly and quantification by RNA-Seq reveals unannotated transcripts and isoform switching during cell differentiation. *Nat Biotechnol* **28**: 511–515.
Van den Bergh, B., Fauvart, M., and Michiels, J. (2017) Formation, physiology, ecology, evolution and clinical importance of bacterial persisters. *FEMS Microbiol Rev* **41**: 219–251.
Wang, X., Kim, Y., Ma, Q., Hong, S.H., Pokusaeva, K., Sturino, J.M., and Wood, T.K. (2010) Cryptic prophages help bacteria cope with adverse environments. *Nat Commun* **1**: 147.
Wang, X., Kim, Y., and Wood, T.K. (2009) Control and benefits of CP4-57 Prophage excision in *Escherichia coli* biofilms. *ISME J* **3**: 1164–1179.
Wood, T.K., and Song, S. (2020) Forming and waking dormant cells: the ppGpp ribosome dimerization persister model. *Biofilm* **2**: 100018.
Yamasaki, R., Song, S., Benedik, M.J., and Wood, T.K. (2020) Persister cells resuscitate using membrane sensors that activate chemotaxis, lower cAMP levels, and revive ribosomes. *iScience* **23**: 100792.
Yeom, J., and Groisman, E.A. (2021) Reduced ATP-dependent proteolysis of functional proteins during nutrient limitation speeds the return of microbes to a growth state. *Sci Signal* **14**: eabc4235.
Yin, X., Wu Orr, M., Wang, H., Hobbs, E.C., Shabalina, S.A., and Storz, G. (2019) The small protein MgtS and small RNA MgrR modulate the PitA phosphate symporter to boost intracellular magnesium levels. *Mol Microbiol* **111**: 131–144.
Yu, W., Li, D., Li, H., Tang, Y., Tang, H., Ma, X., and Liu, Z. (2020) Absence of tmRNA increases the persistence to Cefotaxime and the intercellular accumulation of metabolite GlcNAc in *Aeromonas veronii*. *Front Cell Infect Microbiol* **10**: 44.
Zhao, Y., Lv, B., Sun, F., Liu, J., Wang, Y., Gao, Y., *et al*. (2020) Rapid freezing enables aminoglycosides to eradicate bacterial Persisters via enhancing Mechanosensitive Channel MscL-mediated antibiotic uptake. *mBio* **11**: e03239-03219.
Zheng, E.J., Stokes, J.M., and Collins, J.J. (2020) Eradicating bacterial persisters with combinations of strongly and weakly metabolism-dependent antibiotics. *Cell Chem Biol* **27**: P1544–1552.E1543.

Supporting Information

Additional Supporting Information may be found in the online version of this article at the publisher's web-site:

Appendix S1. Supplementary Information.
File S1. Supplementary Files.

© 2021 Society for Applied Microbiology and John Wiley & Sons Ltd., *Environmental Microbiology*